Available online at www.sciencedirect.com
SCIENCE DIRECT
ELSEVIER
Composites: Part B 37 (2006) 26–36
composites Part B: engineering
www.elsevier.com/locate/compositesb

Buckling analyses of composite laminate skew plates with material nonlinearity

Hsuan-Teh Hu*, Chia-Hao Yang, Fu-Ming Lin

Department of Civil Engineering, National Cheng Kung University, Tainan, Taiwan 701, ROC

Received 21 October 2004; revised 14 May 2005; accepted 16 May 2005
Available online 26 July 2005

Abstract

A nonlinear material constitutive model, including a nonlinear in-plane shear formulation and the Tsai–Wu failure criterion, for fiber–composite laminate materials is employed to carry out finite element buckling analyses for composite laminate skew plates under uniaxial compressive loads. The influences of laminate layup, plate skew angle and plate aspect ratio on the buckling resistance of composite laminate skew plates are presented. Comparing with the linearized buckling loads of the skew plates, one can observer that the nonlinear in-plane shear together with the failure criterion have significant influence on the ultimate loads of the composite laminate skew plates with $[\pm\theta]_{10S}$ and $[\pm\theta/90/0]_{5S}$ layups but not the $[\alpha/0]_{10S}$ layup.

Keywords: B. Buckling; C. Finite element analysis; Skew plate

1. Introduction

Due to light weight and high strength, the use of fiber–composite laminate materials has been increased rapidly in recent year. The composite laminate plates in service are commonly subjected to compressive forces that may cause buckling. Hence, structural instability becomes a major concern in safe and reliable designs of the composite plates. In the literature, most stability studies of fiber–composite laminate plates have been focused on the rectangular plates [1–10]. Less attention has been paid to the skew laminate plates [11–15]. It is known that the buckling resistance of rectangular composite laminate plates depends on end conditions [4,8], ply orientations [1,2,4,5,8,9], and geometric variables such as aspect ratio, thickness and cutout [3,4,6–8,10]. For skew composite plates, the plate skew angle, α (Fig. 1), should also be a key factor influencing the buckling resistance of the plates [11–15]. It is known that unidirectional fibrous composites exhibit severe nonlinearity in in-plane shear stress-strain relation [16,17]. As a result, the buckling resistance of composite plates is also influenced by the nonlinear behavior of the materials [18].

In this paper, a material model including the nonlinear in-plane shear and the Tsai–Wu failure criterion [19] is reviewed first. Then, nonlinear buckling analyses for simply supported composite skew plates under uniaxial compressive force N (Fig. 1) are carried out using the ABAQUS finite element program [20]. The plates in analysis have various laminate layups, plate skew angles and plate aspect ratios. Numerical results for the material nonlinear buckling behavior of these composite plates are compared with those using linear material properties. Through this study, the influences of laminate layups, plate skew angles and plate aspect ratios on the buckling resistance of skew composite plates are demonstrated.

2. Nonlinear material model for composite materials

2.1. Constitutive modeling of lamina

For fiber–composite laminate materials (Fig. 2), each lamina can be considered as an orthotropic layer in a plane stress condition. Let us define $\Delta\{\sigma'\}=\Delta\{\sigma_1,\sigma_2,\tau_{12}\}^{\mathrm{T}}$, $\Delta\{\tau_t'\}=\Delta\{\tau_{13},\tau_{23}\}^{\mathrm{T}}$, $\Delta\{\varepsilon'\}=\Delta\{\varepsilon_1,\varepsilon_2,\gamma_{12}\}^{\mathrm{T}}$, $\Delta\{\gamma_t'\}=\Delta\{\gamma_{13},\gamma_{23}\}^{\mathrm{T}}$. Then the incremental stress-strain relations for

* Corresponding author. Tel.: +886 6 2757575x63168; fax: +886 6 2358542.
E-mail address: hthu@mail.ncku.edu.tw (H.-T. Hu).

1359-8368/$ - see front matter © 2005 Elsevier Ltd. All rights reserved.
doi:10.1016/j.compositesb.2005.05.004

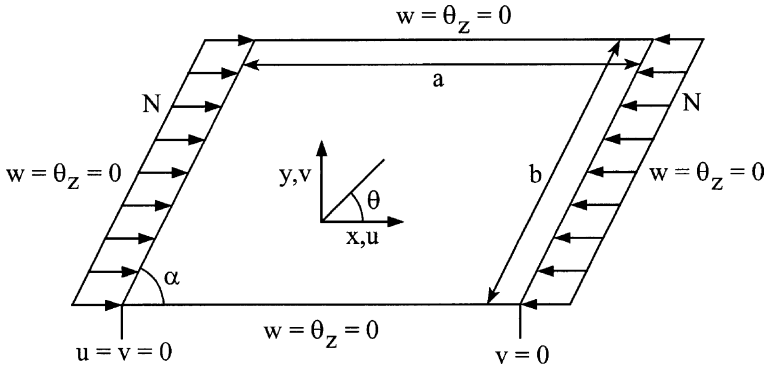

Fig. 1. Composite laminate skew plate with simply supported edge condition.

a linear orthotropic lamina in the material coordinates (1,2,3) can be written as

$$\Delta\{\sigma'\} = [Q_1']\Delta\{\varepsilon'\} \tag{1}$$

$$\Delta\{\tau_t'\} = [Q_2']\Delta\{\gamma_t'\} \tag{2}$$

$$[Q_1'] = \begin{bmatrix} \dfrac{E_{11}}{1-\nu_{12}\nu_{21}} & \dfrac{\nu_{12}E_{22}}{1-\nu_{12}\nu_{21}} & 0 \\ \dfrac{\nu_{21}E_{11}}{1-\nu_{12}\nu_{21}} & \dfrac{E_{22}}{1-\nu_{12}\nu_{21}} & 0 \\ 0 & 0 & G_{12} \end{bmatrix} \tag{3}$$

$$[Q_2'] = \begin{bmatrix} \alpha_1 G_{13} & 0 \\ 0 & \alpha_2 G_{23} \end{bmatrix} \tag{4}$$

where α_1 and α_2 are the shear correction factors [21] and are taken to be 0.83 in this study.

It is known that unidirectional fibrous composites exhibit severe nonlinearity in in-plane shear stress-strain relation [16]. Though deviation from linearity is also observed in transverse loading direction, i.e. 2-direction, the degree of this nonlinearity is not comparable to that in the in-plane shear. Therefore, it has been suggested that the nonlinearity associated with the transverse loading direction could be ignored for graphite/epoxy and boron/epoxy [17]. To model the nonlinear in-plane shear behavior, the nonlinear strain-stress relation for a composite lamina suggested by Hahn and Tsai [16] is adopted in this study, which is given as follows:

$$\begin{Bmatrix} \varepsilon_1 \\ \varepsilon_2 \\ \gamma_{12} \end{Bmatrix} = \begin{bmatrix} \dfrac{1}{E_{11}} & -\dfrac{\nu_{21}}{E_{22}} & 0 \\ -\dfrac{\nu_{12}}{E_{11}} & \dfrac{1}{E_{22}} & 0 \\ 0 & 0 & \dfrac{1}{G_{12}} \end{bmatrix} \begin{Bmatrix} \sigma_1 \\ \sigma_2 \\ \tau_{12} \end{Bmatrix} + S_{6666}\tau_{12}^2 \begin{Bmatrix} 0 \\ 0 \\ \tau_{12} \end{Bmatrix} \tag{5}$$

In this model only one constant S_{6666} is required to account for the in-plane shear nonlinearity. The value of S_{6666} can be determined by a curve fit to various off-axis tension test data [16]. Inverting and differentiating Eq. (5), we obtain the nonlinear incremental constitutive matrix for the lamina as follows:

$$[Q_1'] = \begin{bmatrix} \dfrac{E_{11}}{1-\nu_{12}\nu_{21}} & \dfrac{\nu_{12}E_{22}}{1-\nu_{12}\nu_{21}} & 0 \\ \dfrac{\nu_{21}E_{11}}{1-\nu_{12}\nu_{21}} & \dfrac{E_{22}}{1-\nu_{12}\nu_{21}} & 0 \\ 0 & 0 & \dfrac{1}{1/G_{12}+3S_{6666}\tau_{12}^2} \end{bmatrix} \tag{6}$$

The validity of using Eq. (6) to model the nonlinear in-plane shear has been demonstrated by Hahn and Tsai [16] and is not repeated here. Furthermore, it is assumed that the transverse shear stresses always behave linearly and do not affect the nonlinear behavior of in-plane shear. Hence, the same shear correction factors and shear moduli for transverse shear as those given in Eq. (4) also apply to the cases of nonlinear in-plane shear.

2.2. Failure criterion and degradation of stiffness

Among existing failure criteria, the Tsai–Wu criterion [19] has been extensively used in literature and it is adopted in this analysis. Under plane stress conditions, this failure criterion has the following form:

$$F_1\sigma_1 + F_2\sigma_2 + F_{11}\sigma_1^2 + 2F_{12}\sigma_1\sigma_2 + F_{22}\sigma_2^2 + F_{66}\tau_{12}^2 = 1 \tag{7}$$

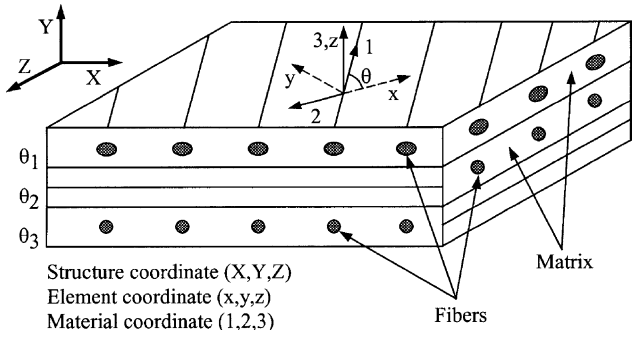

Fig. 2. Material, element and structure coordinates of fiber–composite laminate materials.

and

$$F_1 = \frac{1}{\bar{X}} + \frac{1}{\bar{X}'}, \qquad F_2 = \frac{1}{\bar{Y}} + \frac{1}{\bar{Y}'},$$

$$F_{11} = \frac{-1}{\bar{X}\bar{X}'}, \qquad F_{22} = \frac{-1}{\bar{Y}\bar{Y}'}, \qquad F_{66} = \frac{1}{\bar{S}^2}.$$

The $\bar{X}$, $\bar{Y}$ and $\bar{X}'$, $\bar{Y}'$ are the lamina longitudinal and transverse strengths in tension and compression, respectively, and $\bar{S}$ is the shear strength of the lamina. Though the stress interaction term F_{12} in Eq. (7) is difficult to be determined, it has been suggested by Narayanaswami and Adelman [22] that F_{12} can be set equal to zero for practical engineering applications. Therefore, $F_{12}=0$ is used in this investigation.

During the numerical calculation, incremental loading is applied to composite plates until failures in one or more of individual plies are indicated according to Eq. (7). Since the Tsai–Wu criterion does not distinguish failure modes, the following two rules are used to determine whether the ply failure is caused by resin fracture or fiber breakage [23]:

(1) If a ply fails but the stress in the fiber direction remains less than the uniaxial strength of the lamina in the fiber direction, i.e. $\bar{X}' < \sigma_1 < \bar{X}$, the ply failure is assumed to be resin induced. Consequently, the laminate loses its capability to support transverse and shear stresses, but remains to carry longitudinal stress. In this case, the constitutive matrix of the lamina becomes

$$[Q_1'] = \begin{bmatrix} E_{11} & 0 & 0 \\ 0 & 0 & 0 \\ 0 & 0 & 0 \end{bmatrix} \tag{8}$$

(2) If a ply fails with σ_1 exceeding the uniaxial strength of the lamina, the ply failure is caused by the fiber breakage and a total ply rupture is assumed. In this case, the constitutive matrix of the lamina becomes

$$[Q_1'] = \begin{bmatrix} 0 & 0 & 0 \\ 0 & 0 & 0 \\ 0 & 0 & 0 \end{bmatrix} \tag{9}$$

The ABAQUS program does not have the aforementioned nonlinear constitutive model for fiber–composite laminate materials in material library. Hence, these nonlinear constitutive equations for the composite lamina are coded in FORTRAN language as a subroutine and linked to the ABAQUS program.

2.3. Constitutive modeling of composite shell section

The elements used in the finite-element analyses are eight-node isoparametric shell elements with six degrees of freedom per node (three displacements and three rotations). The formulation of the shell allows transverse shear deformation and these shear flexible shells can be used for both thick and thin shell analysis [20]. During a finite element analysis, the constitutive matrix of composite materials at the integration points of shell elements must be calculated before the stiffness matrices are assembled from the element level to the structural level. For composite materials, the incremental constitutive equations of a lamina in the element coordinates (x,y,z) can be written as:

$$\Delta\{\sigma\} = [Q_1]\Delta\{\varepsilon\} \tag{10}$$

$$\Delta\{\tau_t\} = [Q_2]\Delta\{\gamma_t\} \tag{11}$$

where $\Delta\{\sigma\}=\Delta\{\sigma_x,\sigma_y,\tau_{xy}\}^{\mathrm{T}}$, $\Delta\{\tau_t\}=\Delta\{\tau_{xz},\tau_{yz}\}^{\mathrm{T}}$, $\Delta\{\varepsilon\}=\Delta\{\varepsilon_x,\varepsilon_y,\gamma_{xy}\}^{\mathrm{T}}$, $\Delta\{\gamma_{\mathrm{t}}\}=\Delta\{\gamma_{xz},\gamma_{yz}\}^{\mathrm{T}}$, and

$$[Q_1] = [T_1]^{\mathrm{T}}[Q_1'][T_1] \tag{12}$$

$$[Q_2] = [T_2]^{\mathrm{T}}[Q_2'][T_2] \tag{13}$$

$$[T_1] = \begin{bmatrix} \cos^2\theta & \sin^2\theta & \sin\theta\cos\theta \\ \sin^2\theta & \cos^2\theta & -\sin\theta\cos\theta \\ -2\sin\theta\cos\theta & 2\sin\theta\cos\theta & \cos^2\theta-\sin^2\theta \end{bmatrix} \tag{14}$$

$$[T_2] = \begin{bmatrix} \cos\theta & \sin\theta \\ -\sin\theta & \cos\theta \end{bmatrix} \tag{15}$$

The θ is measured counterclockwise from the element local x-axis to the material 1-axis (Fig. 2). Assume $\Delta\{\varepsilon_{\mathrm{o}}\}=\Delta\{\varepsilon_{\mathrm{xo}},\varepsilon_{\mathrm{yo}},\gamma_{\mathrm{xyo}}\}^{\mathrm{T}}$ are the incremental in-plane strains at the mid-surface of the shell section and $\Delta\{\kappa\}=\Delta\{\kappa_x,\kappa_y,\kappa_{xy}\}^{\mathrm{T}}$ are the incremental curvatures. The incremental in-plane strains at a distance z from the mid-surface of the shell section become

$$\Delta\{\varepsilon\} = \Delta\{\varepsilon_o\} + z\Delta\{\kappa\} \tag{16}$$

Let h be the total thickness of the composite shell section, the incremental stress resultants, $\Delta\{N\}=\Delta\{N_x,N_y,N_{xy}\}^{\mathrm{T}}$, $\Delta\{\mathrm{M}\}=\Delta\{M_x,M_y,M_{xy}\}^{\mathrm{T}}$ and $\Delta\{\mathrm{V}\}=\Delta\{V_x,V_y\}$, can be defined as:

$$\begin{Bmatrix} \Delta\{N\} \\ \Delta\{M\} \\ \Delta\{V\} \end{Bmatrix} = \int_{-h/2}^{h/2} \begin{Bmatrix} \Delta\{\sigma\} \\ z\Delta\{\sigma\} \\ \Delta\{\tau_t\} \end{Bmatrix} \mathrm{d}z$$

$$= \int_{-h/2}^{h/2} \begin{bmatrix} [Q_1] & z[Q_1] & [0] \\ z[Q_1] & z^2[Q_1] & [0] \\ [0]^{\mathrm{T}} & [0]^{\mathrm{T}} & [Q_2] \end{bmatrix} \begin{Bmatrix} \Delta\{\varepsilon_o\} \\ \Delta\{\kappa\} \\ \Delta\{\gamma_t\} \end{Bmatrix} \tag{17}$$

where [0] is a 3 by 2 null matrix.

For the nonlinear material case, the $[Q_1']$ matrix in Eq. (12) can be taken from Eqs. (6), (8) or (9) and the incremental stress resultants of Eq. (17) can be obtained by

a numerical integration through the thickness of the composite shell section. For the linear material case, the $[Q_1']$ matrix used in Eq. (12) is taken from Eq. (3) and the incremental stress resultants of the shell section can be written as a summation of integrals over the n laminae in the following form:

$$\begin{Bmatrix} \Delta\{N\} \\ \Delta\{M\} \\ \Delta\{V\} \end{Bmatrix} = \left(\sum_{j=1}^{n} \begin{bmatrix} (z_{jt}-z_{jb})[Q_1] & \frac{1}{2}(z_{jt}^2-z_{jb}^2)[Q_1] & [0] \\ \frac{1}{2}(z_{jt}^2-z_{jb}^2)[Q_1] & \frac{1}{3}(z_{jt}^3-z_{jb}^3)[Q_1] & [0] \\ [0]^{\mathrm{T}} & [0]^{\mathrm{T}} & (z_{jt}-z_{jb})[Q_2] \end{bmatrix} \right) \begin{Bmatrix} \Delta\{\varepsilon_o\} \\ \Delta\{\kappa\} \\ \Delta\{\gamma_t\} \end{Bmatrix} \tag{18}$$

where z_{jt} and z_{jb} are distances from the mid-surface of the section to the top and the bottom of the jth layer respectively.

Prior to numerical analyses, the ABAQUS program has been employed to analyze the buckling of composite cylindrical panels with cutout and buckling of isotropic skew plates. These solutions are compared with known benchmark solutions [24,25] and satisfactory results are obtained [26].

3. Nonlinear finite element analysis

In the ABAQUS finite element program, the nonlinear response of a structure is modeled by an updated Lagrangian formulation and a modified Riks nonlinear incremental algorithm [20] can be used to construct the equilibrium solution path. To model bifurcation from the prebuckling path to the postbuckling path, geometric imperfections of composite plates are introduced by superimposing a small fraction of the lowest eigenmode, determined by a linearized buckling analysis, to the original nodal coordinates of plate as

$$\{I\} = \{\phi\} + \beta h\{\psi\} \tag{19}$$

where $\{I\}$ represents the vector containing imperfect nodal coordinates of the plate, $\{\phi\}$ is the vector containing original nodal coordinates of the plate, $\{\psi\}$ is the normalized lowest eigenmode, and β is a scaling coefficient. Based on the results of various imperfection analyses [27], it is decided to use $\beta = 0.005$ throughout the numerical analyses.

4. Numerical analyses

4.1. Verification of the proposed material constitutive models

The validity of the nonlinear material constitutive models to simulate the behavior of composite materials has been examined in this section by comparing with the experiment results performed by Soutis [28]. The tested specimens have two types of laminate layups, i.e. $[0]_{16}$ and $[(\pm 45/0_2)_3]_S$, and are both subjected to uniaxial compressive force in the longitudinal direction (Fig. 3). The two loading edges of the laminates are assumed to be fixed and the remaining two edges are free. The laminates are consisted of T800/924C carbon-fibre/epoxy composite with the following material properties: $E_{11} = 168$ GPa, $E_{22} = 9.25$ GPa, $\nu_{12} = 0.35$, $G_{12} = 6$ GPa, $S_{6666} = 7 \times 10^{-20}$ $(\mathrm{Pa})^{-3}$, $\bar{X} = 2.32$ GPa, $\bar{X}' = -1.62$ GPa, $\bar{Y} = 63$ MPa, $\bar{Y}' = -63$ MPa, $\bar{S} = 105$ MPa. The thickness of each ply is 0.125 mm. Since the stress field is uniform throughout the specimen, only one shell element is used to model the entire composite laminate in the numerical analysis.

Fig. 3 also shows the stress versus strain curves of the composite laminates in the longitudinal direction. It can be observed that the correlations are quite good between the numerical results and the experimental data whether the shear stresses in the laminate are significant (i.e. $[(\pm 45/0_2)_3]_S$ layup) or not (i.e., $[0]_{16}$ layup). The predicted ultimate strength 1.6 GPa for $[0]_{16}$ laminate is in good agreement with the experimental ultimate strength 1.55 GPa. The error is only about 3.2%. In addition, the predicted ultimate strength 0.81 GPa for $[(\pm 45/0_2)_3]_S$ laminate is also in good

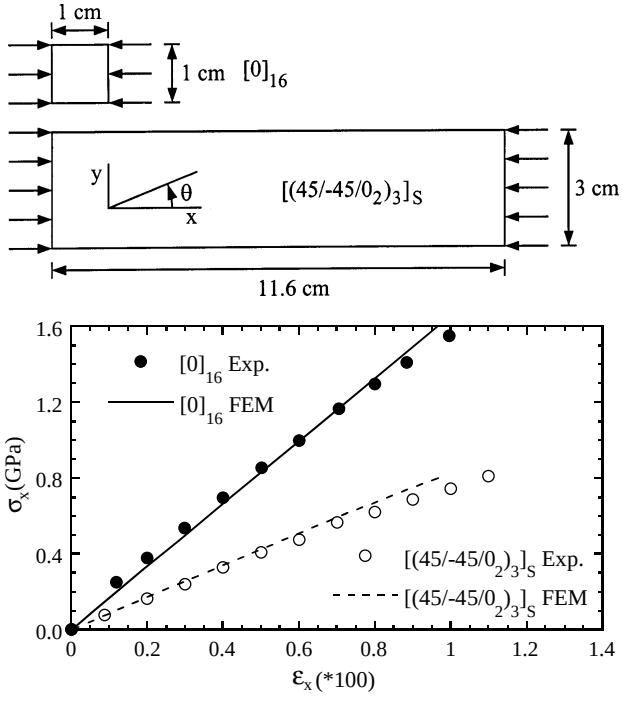

Fig. 3. Comparisons of numerical and experimental results.

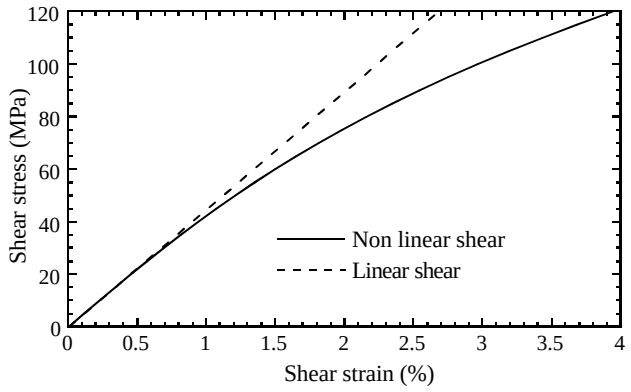

Fig. 4. In-plane shear stress–strain curves for composite lamina.

agreement with the experimental ultimate strength 0.80 GPa. The error is only about 1.3%. Hence, the proposed material constitutive models are proved to be able to simulate the nonlinear behavior of composite materials correctly. More numerical verifications of the proposed nonlinear constitutive material models against other experimental data have also been done by the author [29,30] and are not duplicated here.

4.2. Composite laminate skew plates with $[\pm\theta]_{10S}$ layup

In this section composite laminate plates subjected to uniaxial compressive force N per unit length in x direction as shown in Fig. 1 are analyzed. These plates are simply supported at the edges and the edge conditions prevent out of plane displacement w but allow in-plane movements u and v. The width 'b' of these plates is fixed to 10 cm and the length 'a' of the plates varies between 5 cm and 20 cm. The thickness of the plates is 0.5 cm and the skew angle α varies between 50° and 90°. The laminate layup of the plates is $[\pm\theta]_{10S}$ and the ply constitutive properties are $E_{11}=128$ GPa, $E_{22}=11$ GPa, $\nu_{12}=0.25$, $G_{12}=G_{13}=4.48$ GPa, $G_{23}=1.53$ GPa, $S_{6666}=7.31$ $(\text{GPa})^{-3}$, $\bar{X}=-\bar{X}'=1450$ MPa, $\bar{Y}=52$ MPa, $\bar{Y}'=-206$ MPa and $S=93$ MPa. The linear and nonlinear in-plane shear stress-strain curves are shown in Fig. 4. In the finite element analysis, no symmetry simplifications are made. Based on past experience [14], a 10×10 finite element mesh (100 elements) is used to model the plates.

Fig. 5 shows the load-displacement curves for composite laminate skew plates with aspect ratio $a/b=1$, skew angle $\alpha=50°$ and $[\pm\theta]_{10S}$ laminate layup. The N is the force per unit length in x direction (positive value means compression) applied to the edge and u is the associated end displacement (positive value means end extension and negative value means end shortening). For plates with $[0/-0]_{10S}$ and $[90/-90]_{10S}$ layups, it can be seen that the curves computed by using linear and nonlinear in-plane shear formulations are very close. This is because that all the fibers are parallel or normal to the loading direction and shear stress is insignificant in the plates. For the analyses

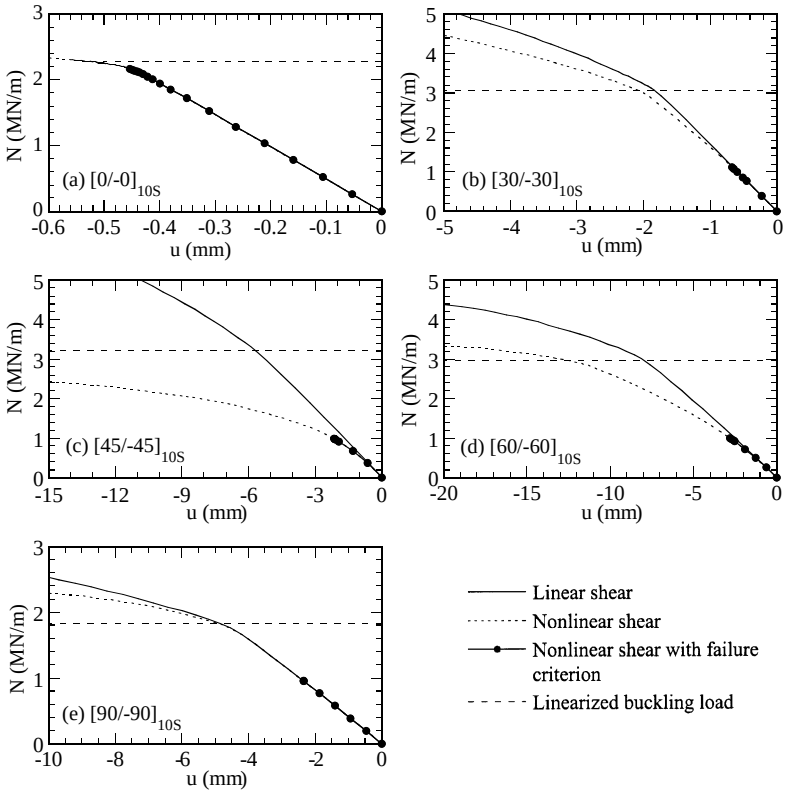

Fig. 5. Load–displacement curves for composite laminate skew plate with $[\pm\theta]_{10S}$ layup under uniaxial compression ($a/b=1$, $\alpha=50°$).

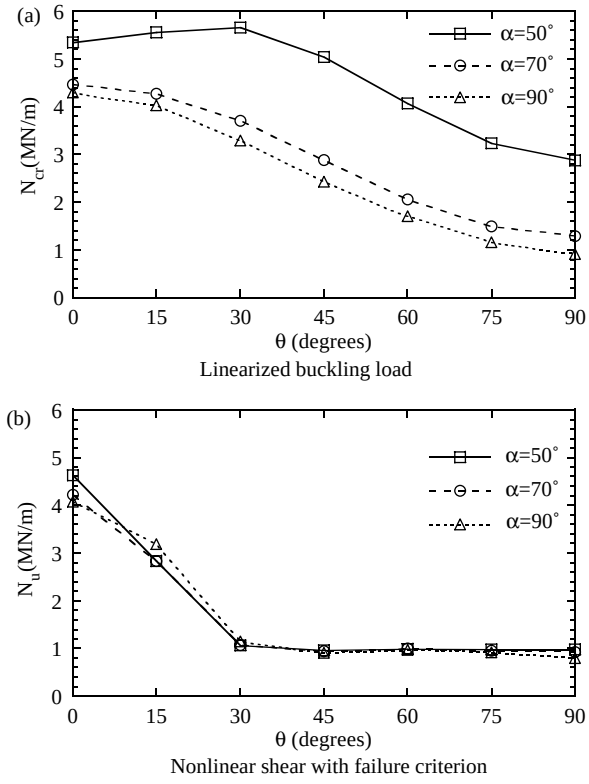

Fig. 6. Effect of skew angle α and material nonlinearity on buckling loads of composite laminate skew plate with $[\pm\theta]_{10S}$ layup ($a/b=0.5$).

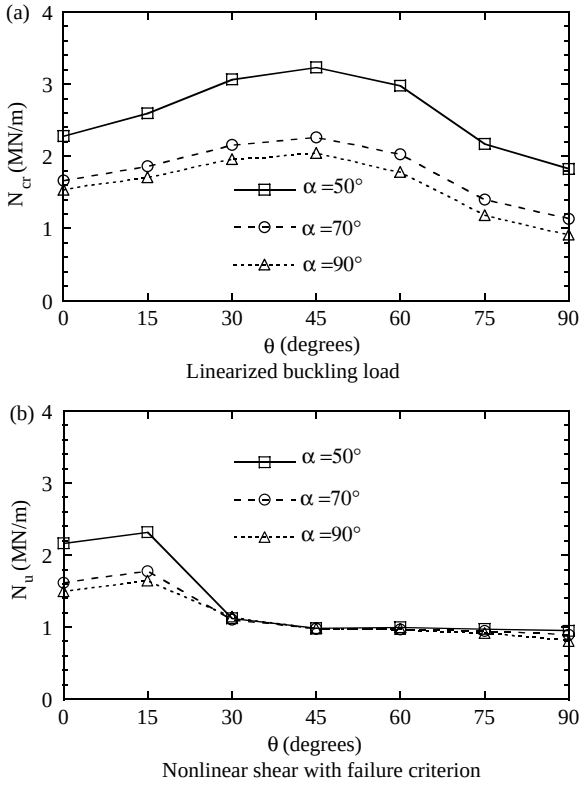

Fig. 7. Effect of skew angle α and material nonlinearity on buckling loads of composite laminate skew plate with $[\pm\theta]_{10S}$ layup ($a/b=1$).

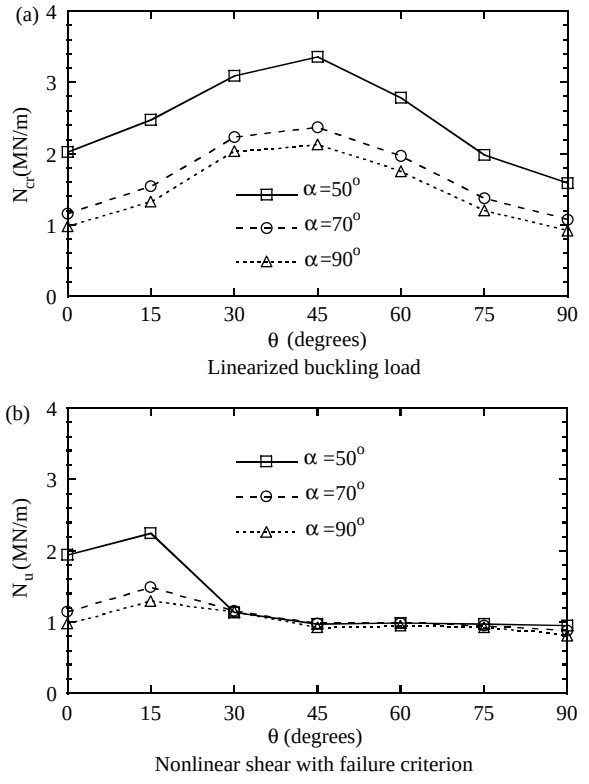

Fig. 8. Effect of skew angle α and material nonlinearity on buckling loads of composite laminate skew plate with $[\pm\theta]_{10S}$ layup ($a/b=2$).

carried out using the nonlinear in-plane shear formulation together with the Tsai–Wu failure criterion, the composite plates behave almost linearly until sudden collapses of the plates occur. The predicted ultimate load is about 95% of the linearized buckling load for plate with $[0/-0]_{10S}$ layup and is about 52% for plate with $[90/-90]_{10S}$ layup.

For skew plate with $[30/-30]_{10S}$ and $[60/-60]_{10S}$ layups, the fiber angles are away from the loading or the transverse loading directions. In these plates, shear stress start to develop and the curves with nonlinear shear formulation show moderate deviations from the curves with linear shear formulation. For the analyses carried out using the nonlinear in-plane shear formulation together with the Tsai–Wu criterion, the predicted ultimate load is about 37% of the linearized buckling load for plate with $[30/-30]_{10S}$ layup and about 34% for plate with $[60/-60]_{10S}$ layup.

For plate with $[45/-45]_{10S}$ layup, each lamina is subjected to severe shear loading. With the nonlinear in-plane shear formulation alone, the plate exhibit significantly nonlinear behavior throughout the entire loading stage. The load carrying capacity for the plate with the nonlinear in-plane shear formulation is much less than that with the linear shear formulation. In addition, the predicted ultimate load is only about 30% of the linearized buckling load, which is the lowest percentage value among all the plates in analysis.

The load-displacement curves for $[\pm\theta]_{10S}$ composite laminate skew plates with other aspect ratios ($a/b=0.5$, 2)

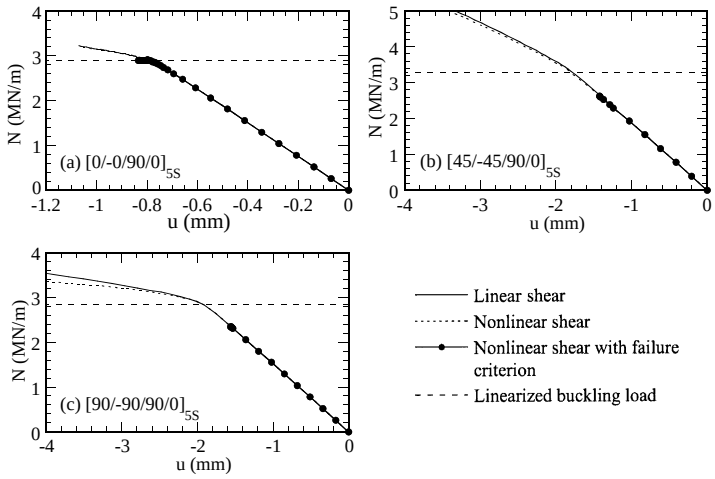

Fig. 9. Load–displacement curves for composite laminate skew plate with $[\pm\theta/90/0]_{5S}$ layup under uniaxial compression ($a/b=1$, $\alpha=50°$).

and skew angles ($\alpha=70°$, 90°) show similar trends as those in Fig. 5 and are not duplicated here. Figs. 6–8 show the effect of skew angle α and material nonlinearity on buckling loads of composite laminate skew plate with $[\pm\theta]_{10S}$ layup. From Figs. 6(a), 7(a) and 8(a), it can be observed that with the same laminate layup and the same plate skew angle, the linearized buckling load N_{cr} increases with the decrease of plate aspect ratio. In addition, with the same laminate layup and plate aspect ratio, the linearized buckling load increases with the decreasing of angle α. Furthermore, the curve with $\alpha=70°$ is closer to that with $\alpha=90°$ than to that with $\alpha=50°$. It can be concluded that the larger the α angle, the smaller the increasing/decreasing rate in N_{cr}. When the plate aspect ratio a/b is small (say $a/b\leq0.5$), the optimal fiber angle θ for skew plate with $[\pm\theta]_{10S}$ laminate layup seems to close to 0°. This phenomenon is more prominent when the skew angle α is equal to or greater than 70°. On the other hand, when the plate aspect ratio a/b is large (say $a/b\geqq1$), the optimal fiber angle θ seems to be around 45°. This phenomenon seems to be independent on the skew angle α.

From Figs. 6(b), 7(b) and 8(b), it can be seen that the ultimate load N_u seems to be independent on the fiber angle θ, the skew angle α and the aspect ratio a/b when the fiber angle $\theta\geqq30°$. When $\theta\leq30°$ and a/b is small (say $a/b\leq0.5$), the ultimate load of the skew plate seems to be insensitive to the skew angle α. When $\theta\leq30°$ and a/b is large (say $a/b\geqq1$), the ultimate load of the skew plate increases with the decreasing of angle α. When the plate aspect ratio a/b is small (say $a/b\leq0.5$), the optimal fiber angle θ seems to be 0°. When the plate aspect ratio a/b is large (say $a/b\geqq1$), the optimal fiber angle θ seems to be around 15°.

Comparing Figs. 6(b), 7(b) and 8(b) with Figs. 6(a), 7(a) and 8(a), we can observe that when the angle θ is close to 0°, the effect of nonlinear shear with failure criterion seems to be insignificant. When the angle θ is close to 90°, the effect of nonlinear shear with failure criterion is prominent for plate with small angle α (say $\alpha=50°$). This effect is less significant for plate with large angle α (say $\alpha=90°$). When the angle θ varies between 15° and 75°, the influence of the nonlinear shear with failure criterion on the ultimate load of the skew plate is significant, especially for plates with small angle α. This conclusion is valid whether the plate aspect ratio is small or large.

4.3. Composite laminate skew plates with $[\pm\theta/90/0]_{5S}$ layup

In this section composite laminate skew plates similar to those in previous section are analyzed. However, the laminate layup is changed to $[\pm\theta/90/0]_{5S}$. Fig. 9 shows the load-displacement curves for composite laminate skew plates with aspect ratio $a/b=1$ and skew angle $\alpha=50°$. For plates with $[0/-0/90/0]_{5S}$ and $[90/-90/90/0]_{5S}$ layups, it can be seen that the curves computed by using linear and nonlinear in-plane shear formulations again are very close. This is because all the fibers are parallel to or normal to the loading direction and the shear stresses in the plates are insignificant. For plate with $[45/-45/90/0]_{5S}$ layup, we might expect that the nonlinear shear effect to be significant in the plate. However, the curve computed with nonlinear in-plane shear formulation is also very close to that with linear in-plane shear formulation. The reason might be that the fibers in the 0° direction take the major portion of the loading and the shear stresses in the 45° and -45° laminae are not significant enough to cause the difference between the linear and nonlinear shear formulations. As a result, the effect of nonlinear in-plane shear stress is insignificant for the $[\pm\theta/90/0]_{5S}$ composite laminate skew plates. The load-displacement curves for $[\pm\theta/90/0]_{5S}$ composite laminate skew plates with other aspect ratios ($a/b=0.5$, 2) and skew angles ($\alpha=70°$, 90°) show similar trends as those in Fig. 9 and are not duplicated here.

Figs. 10–12 show the effect of skew angle α and material nonlinearity on buckling loads of composite laminate skew plate with $[\pm\theta/90/0]_{5S}$ layup. From Figs. 10(a), 11(a) and 12(a), it can be observed that with the same laminate layup

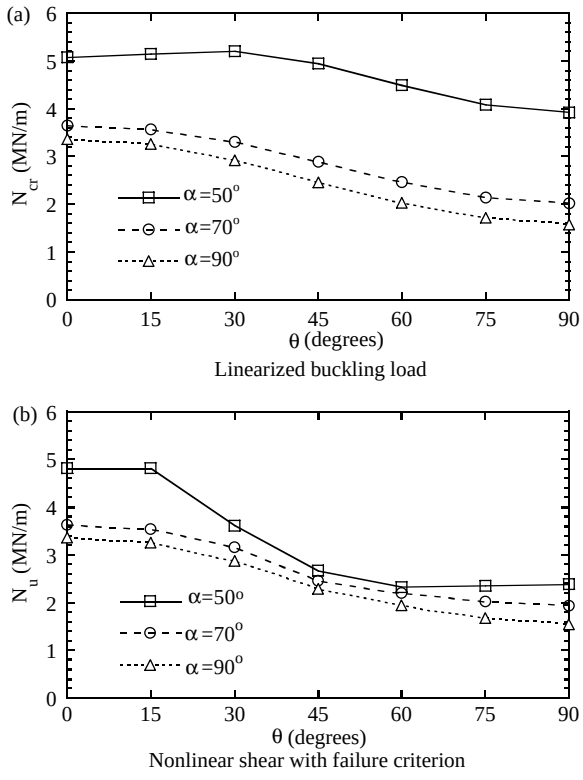

Fig. 10. Effect of skew angle α and material nonlinearity on buckling loads of composite laminate skew plate with $[\pm\theta/90/0]_{5S}$ layup ($a/b=0.5$)

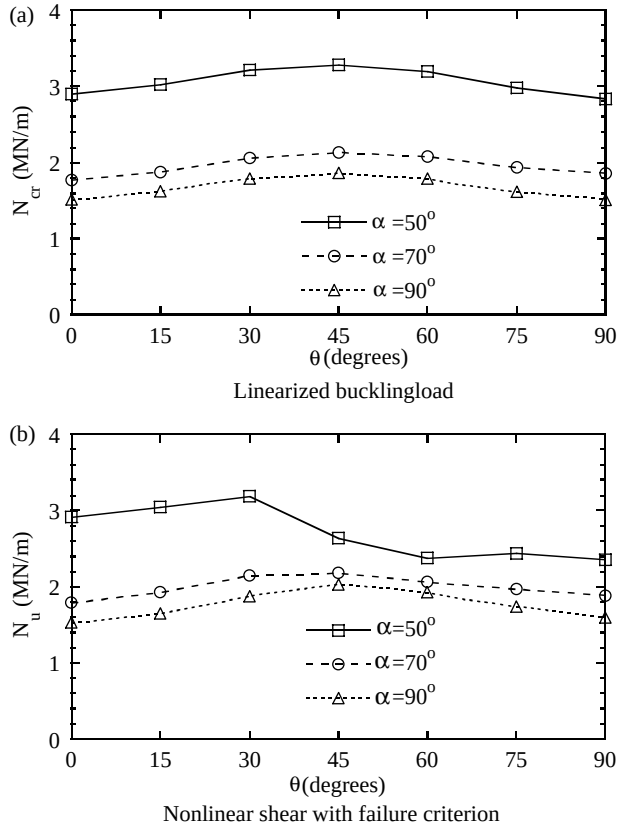

Fig. 11. Effect of skew angle α and material nonlinearity on buckling loads of composite laminate skew plate with $[\pm\theta/90/0]_{5S}$ layup ($a/b=0.5$).

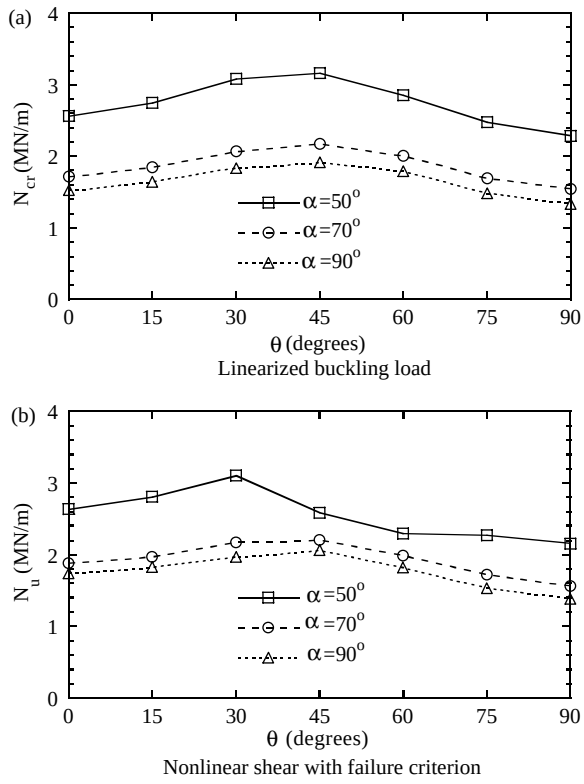

Fig. 12. Effect of skew angle α and material nonlinearity on buckling loads of composite laminate skew plate with $[\pm\theta/90/0]_{5S}$ layup ($a/b=2$).

and the same plate skew angle, the linearized buckling load N_{cr} increases with the decrease of plate aspect ratio. In addition, with the same laminate layup and plate aspect ratio, the linearized buckling load increases with the decreasing of angle α. Furthermore, the curve with $\alpha=70°$ is closer to that with $\alpha=90°$ than to that with $\alpha=50°$. It can be concluded that the larger the α angle, the smaller the increasing/decreasing rate in N_{cr}. When the plate aspect ratio a/b is small (say $a/b\leq 0.5$), the optimal fiber angle θ for skew plate with $[\pm\theta/90/0]_{5S}$ laminate layup seems to close to 0°. This phenomenon is more prominent when the skew angle α is equal to or greater than 70°. On the other hand, when the plate aspect ratio a/b is large (say $a/b\geqq 1$), the optimal fiber angle θ seems to be around 45°. This phenomenon seems to be independent on the skew angle α. Generally the conclusions related to the linearized buckling loads for $[\pm\theta/90/0]_{5S}$ laminate skew plates are similar to those for $[\pm\theta]_{10S}$ laminate skew plates.

From Figs. 10(b), 11(b) and 12(b), it can be seen that with the same laminate layup and the same plate skew angle, the ultimate load N_u increases with the decreasing of plate aspect ratio. In addition, with the same laminate layup and plate aspect ratio, the ultimate load increases with the decreasing of angle α. Furthermore, the curve with $\alpha=70°$ is closer to that with $\alpha=90°$ than to that with $\alpha=50°$. It can be concluded that the larger the α angle, the smaller the increasing/decreasing rate in N_u. When the plate aspect

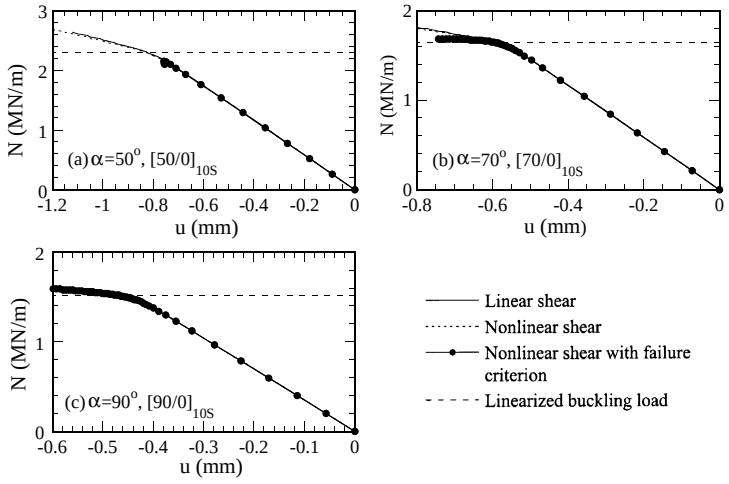

Fig. 13. Load–displacement curves for composite laminate skew plate with $[\alpha/0]_{10S}$ layup under uniaxial compression ($a/b=1$).

ratio a/b is small (say $a/b \leq 0.5$), the optimal fiber angle θ for skew plate with $[\pm\theta/90/0]_{5S}$ laminate layup seems to close to 0°. This phenomenon is more prominent when the skew angle α is equal to or greater than 70°. When the plate aspect ratio a/b is large (say $a/b \geqq 1$), the optimal fiber angle θ seems to be around 30° to 45°.

Comparing Figs. 10(b), 11(b) and 12(b) with Figs. 10(a), 11(a) and 12(a), we can observe that the effect of nonlinear shear with failure criterion is significant for plates with small α angle (say $\alpha \leq 50°$) and is insignificant for plates with large α angle (say $\alpha \geqq 70°$). For plates with small α angle (say $\alpha \leq 50°$), the effect of nonlinear shear with failure criterion is only significant when the fiber angle θ is less than 15°. Comparing the results obtained in this section with those in previous section, we can find that the influence of nonlinear shear with failure criterion on the ultimate loads of laminate skew plates with $[\pm\theta/90/0]_{5S}$ laminate layup is much less than those with $[\pm\theta]_{10S}$ laminate layup. Hence, the former laminate layup is a better design than the latter one in practical engineering applications.

4.4. Composite laminate skew plates with $[a/0]_{10S}$ layup

In this section composite laminate skew plates similar to those in previous sections are analyzed with the laminate layup changed to $[\alpha/0]_{10S}$. For this laminate layup, the fiber directions are all parallel to the edges of the skew plates. Fig. 13 shows the load-displacement curves for plates with aspect ratio $a/b=1$ and plate skew angle $\alpha=50°$, 70°, 90°. From these figures, it can be seen that the curves computed by using linear and nonlinear in-plane shear formulations are almost the same. This is because the fibers in the 0° direction take the major portion of the loading and the shear stresses in the laminae with fibers in α direction are not significant enough to cause the difference between the linear and nonlinear shear formulations. As a result, the effect of nonlinear in-plane shear stress is insignificant for the $[\alpha/0]_{10S}$ composite laminate skew plates.

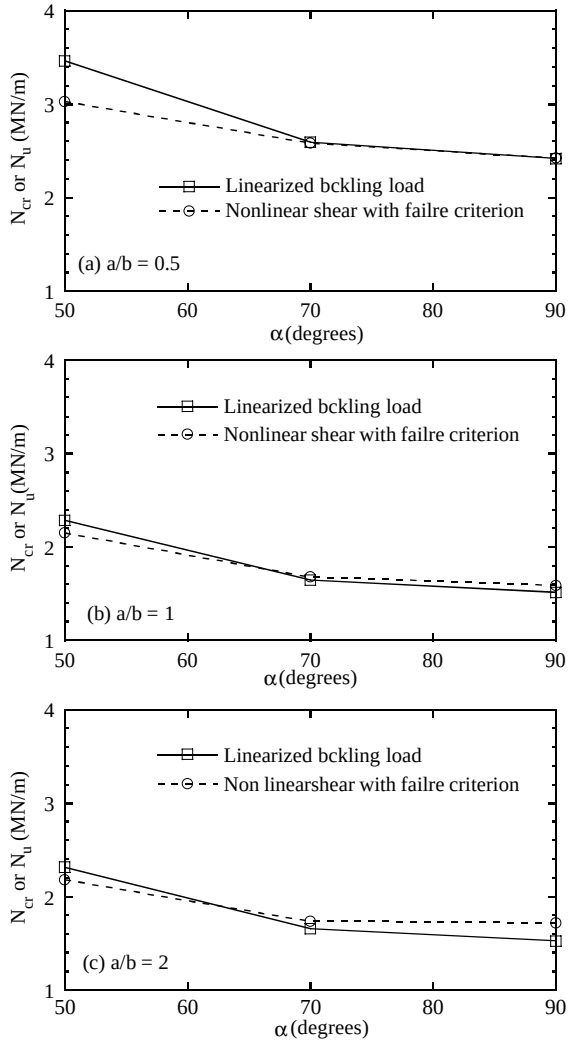

Fig. 14. Effect of skew angle α, aspect ratio a/b and material nonlinearity on buckling loads of composite laminate skew plate with $[\alpha/0]_{10S}$ layup.

Fig. 14 shows the effect of skew angle α, aspect ratio a/b and material nonlinearity on buckling loads of composite laminate skew plate with $[\alpha/0]_{10S}$ layup. It can be seen that the linearized buckling loads N_{cr} of the skew plates again increase with the decreasing of plate aspect ratio a/b and with the decreasing of angle α. In addition, the ultimate loads N_u of the skew plates calculated by the nonlinear shear formulation with Tsai–Wu failure criterion are very close to the linearized buckling loads N_{cr}. Thus, influence of nonlinear shear with failure criterion on the ultimate loads of laminate skew plates with $[\alpha/0]_{10S}$ laminate layup is very limited and material nonlinear buckling analysis of skew plates with this type of laminate layup may be not necessary.

5. Conclusions

Based on the numerical results from the analyses, the following conclusions may be drawn:

(1) No matter of plate aspect ratio and skew angle, nonlinear in-plane shear alone has significant influence on the load-displacement curves of laminate skew plates with $[\pm\theta]_{10S}$ laminate layup. This influence is most significant when θ is equal to 45° and less significant when θ deviates from 45°.
(2) Nonlinear in-plane shear alone has almost no influence on the load-displacement curves of laminate skew plates with $[\pm\theta/90/0]_{5S}$ and $[\alpha/0]_{10S}$ laminate layups.
(3) The linearized buckling loads of the plates with $[\pm\theta]_{10S}$, $[\pm\theta/90/0]_{5S}$ and $[\alpha/0]_{10S}$ laminate layups increase with the decreasing of plate aspect ratio a/b and with the decreasing of angle α.
(4) For skew plates with both $[\pm\theta]_{10S}$ and $[\pm\theta/90/0]_{5S}$ layups, the optimal fiber angle θ for the linearized buckling loads seems to close to 0° when the plate aspect ratio a/b is small (say $a/b \leq 0.5$). However, when the plate aspect ratio a/b is large (say $a/b \geqq 1$), the optimal fiber angle θ for plates with both laminate layups seems to be around 45°.
(5) The influence of the nonlinear shear with failure criterion on the ultimate loads of the laminate skew plates with $[\pm\theta]_{10S}$ laminate layup is significant, especially for plates with small angle α. When the plate aspect ratio a/b is small (say $a/b \leq 0.5$), the optimal fiber angle θ for the ultimate load seems to be 0°. When the plate aspect ratio a/b is large (say $a/b \geqq 1$), the optimal fiber angle θ seems to be around 15°.
(6) The influence of the nonlinear shear with failure criterion on the ultimate loads of the laminate skew plates with $[\pm\theta/90/0]_{5S}$ laminate layup is significant for plates with small α angle (say $\alpha \leq 50°$) and is insignificant for plates with large α angle (say $\alpha \geqq 70°$). When the plate aspect ratio a/b is small (say $a/b \leq 0.5$), the optimal fiber angle θ for the ultimate load seems to close to 0°. When the plate aspect ratio a/b is large (say $a/b \geqq 1$), the optimal fiber angle θ seems to be around 30° to 45°.
(7) The influence of nonlinear shear with failure criterion on the ultimate loads of laminate skew plates with $[\pm\theta/90/0]_{5S}$ laminate layup is much less than those with $[\pm\theta]_{10S}$ laminate layup. Hence, the former laminate layup is a better design than the latter one in practical engineering applications.
(8) The influence of nonlinear shear with failure criterion on the ultimate loads of laminate skew plates with $[\alpha/0]_{10S}$ laminate layup is very limited and material nonlinear buckling analysis of skew plates with this type of laminate layup may be not necessary.

References

[1] Crouzet-Pascal J. Buckling analysis of laminated composite plates. Fibre Sci Technol 1978;11:413–46.
[2] Hirano Y. Optimum design of laminated plates under axial compression. AIAA J 1979;17:1017–9.
[3] Rhodes MD, Mikulas MM, McGowan PE. Effects of orthotropy and width on the compression strength of graphite-epoxy panels with holes. AIAA J 1984;22:1283–92.
[4] Leissa AW. Buckling of laminated composite plates and shell panels, AFWAL-TR-85-3069. Flight Dynamics Laboratory, Air Force Wright Aeronautical Laboratories, Wright-Patterson Air Force Base, Ohio; 1985.
[5] Muc A. Optimal fibre orientation for simply-supported angle-ply plates under biaxial compression. Compos Struct 1988;9:161–72.
[6] Nemeth MP. Buckling behavior of compression-loaded symmetrically laminated angle-ply plates with holes. AIAA J 1988;26:330–6.
[7] Vellaichamy S, Prakash BG, Brun S. Optimum design of cutouts in laminated composite structures. Comput Struct 1990;37:241–6.
[8] Hu H-T, Lin B-H. Buckling optimization of symmetrically laminated rectangular plates with various geometry and end conditions. Compos Sci Technol 1995;55:277–85.
[9] Ari-Gur J, Simonetta SR. Dynamic pulse buckling of rectangular composite plates. Compos Part B: Eng 1997;28:301–8.
[10] Shrivastava AK, Singh RK. Effect of aspect ratio on buckling of composite plates. Compos Sci Technol 1999;59:439–45.
[11] Wang CM, Liew KM, Alwis WAM. Buckling of skew plates and corner condition for simply supported edges. J Eng Mech, ASCE 1992;118:651–62.
[12] Liao C-L, Lee Z-Y. Elastic stability of skew laminated composite plates subjected to biaxial follower forces. Int J Numer Methods Eng 1993;36:1825–47.
[13] Reddy ARK, Palaninathan R. Buckling of laminated skew plates. Thin-Walled Struct 1995;22:241–59.
[14] Hu H-T, Tzeng W-L. Buckling analysis of skew laminate plates subjected to uniaxial inplane loads. Thin-Walled Struct 2000;38:53–77.
[15] Kant T, Babu CS. Thermal buckling analysis of skew fibre-reinforced composite and sandwich plates using shear deformable finite element models. Compos Struct 2000;49:77–85.
[16] Hahn HT, Tsai SW. Nonlinear elastic behavior of unidirectional composite laminae. J Compos Mater 1973;7:102–18.
[17] Jones RM, Morgan HS. Analysis of nonlinear stress-strain behavior of fiber-reinforced composite materials. AIAA J 1977;15:1669–76.
[18] Hu H-T. Buckling analyses of fiber composite laminate plates with material nonlinearity. Finite Elem Anal Design 1995;19:169–79.

[19] Tsai SW, Wu EM. A general theory of strength for anisotropic materials. J Compos Mater 1971;5:58–80.
[20] Hibbitt, Karlsson & Sorensen, Inc. ABAQUS user's manuals and theory manuals, Version 6.2. Rhode Island: Providence; 2002.
[21] Mindlin RD. Influence of rotatory inertia and shear on flexural motions of isotropic elastic plates. J Appl Mech 1951;18:31–8.
[22] Narayanaswami R, Adelman HM. Evaluation of the tensor polynomial and Hoffman strength theories for composite materials. J Compos Mater 1977;11:366–77.
[23] Rowlands RE. Strength (failure) theories and their experimental correlation. In: Sih GC, Skudra AM, editors. Failure mechanics of composites. Amsterdam, The Netherlands: Elsevier; 1985. p. 71–125.
[24] Stanely GM. Continuum-based shell element.PhD Thesis.Department of Mechanical Engineering, Stanford University;1985.
[25] Morley LSD. Skew plates and structures. New York: Macmillan; 1963.
[26] Tzeng W-L. Buckling analysis of laminate parallelogram plates subjected to uniaxial compression. MS Thesis.Department of Civil Engineering, National Cheng Kung University, Tainan, ROC; 1996.
[27] Yang C-H. Numerical analysis of laminate parallelogram plates with material nonlinearity. MS Thesis. Department of Civil Engineering, National Cheng Kung University, Tainan, ROC; 1999.
[28] Soutis C. Measurement of the Static Compressive Strength of Carbon-Fibre/Epoxy Laminates. Composites Science and Technology 1991; 42:373–92.
[29] Lin W-P, Hu H-T. Nonlinear analysis of fiber-reinforced composite laminates subjected to uniaxial tensile load. Journal of Composite Materials 2002;36:1429–50.
[30] Lin W-P, Hu H-T. Parametric study on the failure of fiber-reinforced composite laminates under biaxial tensile load. Journal of Composite Materials 2002;36:1481–504.